POLITECNICO DI TORINO
Repository ISTITUZIONALE

Very High Q-Factor Bandpass Filter Using Additive Manufacturing

Original
Very High Q-Factor Bandpass Filter Using Additive Manufacturing / López-Oliver, E., Tomassoni, C., Addamo, G., Calignano, F., Lumia, M., Peverini, O., Virone, G.. - STAMPA. - 1:(2021), pp. 243-245. (2021 IEEE MTT-S International Microwave Filter Workshop Perugia 17–19 novembre 2021) [10.1109/IMFW49589.2021.9642294].

Availability:
This version is available at: 11583/3017256 since: 2026-10-30T18:23:59Z

Publisher:
Institute of Electrical and Electronics Engineers (IEEE)

Published
DOI:10.1109/IMFW49589.2021.9642294

Terms of use:

This article is made available under terms and conditions as specified in the corresponding bibliographic description in the repository

Publisher copyright
IEEE postprint/Author's Accepted Manuscript

©2021 IEEE. Personal use of this material is permitted. Permission from IEEE must be obtained for all other uses, in any current or future media, including reprinting/republishing this material for advertising or promotional purposes, creating new collecting works, for resale or lists, or reuse of any copyrighted component of this work in other works.

(Article begins on next page)

29 November 2026

Very High Q-Factor Bandpass Filter Using Additive Manufacturing

1st Enrique López-Oliver
University of Perugia
Perugia, Italy
enrique.lopezoliver@unipg.it

2nd Cristiano Tomassoni
University of Perugia
Perugia, Italy
cristiano.tomassoni@unipg.it

3rd Giuseppe Addamo
CNR-IEIIT
Turin, Italy
giuseppe.addamo@ieiit.cnr.it

4th Flaviana Calignano
DIGEP-IAM
Turin, Italy
flaviana.calignano@polito.it

5th Mauro Lumia
CNR-IEIIT
Turin, Italy
mauro.lumia@ieiit.cnr.it

6th Oscar Peverini
CNR-IEIIT
Turin, Italy
oscar.peverini@ieiit.cnr.it

7th Giuseppe Virone
CNR-IEIIT
Turin, Italy
giuseppe.virone@ieiit.cnr.it

***Abstract*—A spherical bandpass filter is presented. The main feature of the proposed filter is the use of the spherical mode TE_{101}, which presents a higher unloaded Q-factor than the fundamental mode and its proximate higher order modes. As a result, in this work, the mode TE_{101} has been exploited in the design of a 2-pole filter with a central frequency at 10 GHz and fractional bandwidth 1.2%. The fabrication has been carried out using the selective laser melting technology in order to exploit the flexibility of additive manufacturing. In particular, two monolithic prototypes have been manufactured. Good agreement between measurements and simulations have been observed, with almost identical results between the two manufactured prototypes, thus proving the repeatability of the process. No tuning screws have been used.**

***Index Terms*—Bandpass filter, spherical cavity, spherical resonator, spherical filter, narrow-band filter, Q-factor, selective laser melting (SLM), additive manufacturing (AM).**

I. Introduction

Generally, waveguide filters are an excellent choice when low insertion loss and high-power handling capabilities are required [1]. In space communications, for instance, it is very important to minimize losses, especially when a filter is positioned in the receiver front-end just after the antenna. Indeed, in this position the signal has not yet been amplified and its power is generally very low. In this case, losses in filters may sensibly decrease the signal-to-noise ratio.

The most exploited geometries are rectangular and circular. Generally, rectangular and circular waveguide filters are used in their fundamental modes, in single or dual/triple mode configuration when compactness is a requirement. On some occasions, higher order modes are exploited. As an example, higher order modes in circular cavity filters (e.g., TE_{113}) are used in space applications for increasing the cavity Q-factor. Another interesting application is for the introduction of transmission zeros (TZs) in filters with in-line geometries. In that case, higher order resonating modes are used for generating the filter poles while the fundamental (nonresonating) mode is exploited for bypassing the resonant modes, thus introducing cross-couplings capable of generating TZs. An example of this is shown in [2], [3] for rectangular TM cavity filters, and in [4]. for dielectric-loaded TM cavity filters. The use of higher order modes has the disadvantage of leading to larger structures, but on the other hand, larger sizes represent an advantage from the point of view of manufacturing tolerances.

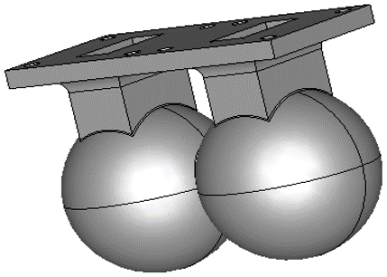

Fig. 1. Cad geometry of the realized 2-order filter.

On the other hand, the recent advances in additive manufacturing (AM) [5] have allowed the manufacturing of filters with non-conventional geometries [6], [7] such as spherical geometries [8], which are more difficult to manufacture by using traditional manufacturing technology. In [8], filters with spherical cavities have been studied in order to take advantage of the high Q-factor of the fundamental mode of the spherical cavity. More recently, the use of a higher order mode (the TM_{211}) was introduced in [9]. In this case, however, the purpose was mostly the suppression of the spurious rather than increasing the Q-factor, indeed the Q-factor of the TM_{211} is quite similar to that of the fundamental spherical mode.

In this paper, for the first time (to the authors knowledge), the spherical mode TE_{101} has been exploited in order to obtain filters with very high Q-factor. Thanks to its particular field distribution that concentrates the field in the center of the cavity minimizing the fields (and then the currents) in the cavity wall, the TE_{101} has indeed an impressive high Q-factor that is almost double the Q-factor of the fundamental spherical mode.

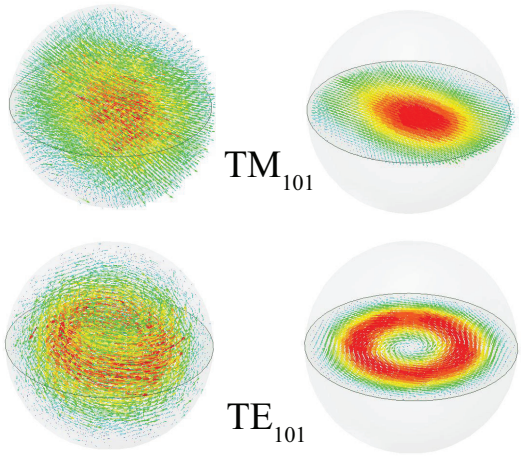

Fig. 2. E-field distribution. TM_{101} mode (above) and TE_{101} mode (below).

This extremely high Q-factor can be exploited for minimizing losses in the design of very narrow-band filters, which are very sensitive to manufacturing tolerances. In fact, filters operating with the TE_{101} mode are larger than that based on fundamental modes and this make the filter less sensitive to manufacturing tolerances. Moreover, the proposed filter has an additional bonus related to the use of higher order modes, i.e., the fact that the fundamental mode introduces TZs, even though their position is not controllable. A view of a two-pole prototype of a spherical filter (Fig. 1), which has been manufactured with the selective laser melting (SLM) technology. Measured results of the fabricated prototypes demonstrate the feasibility of the proposed approach.

II. Cavity Modes

In spherical cavities, the modes are classified into TM_{mnp} and TE_{mnp}. The fundamental mode in a spherical cavity is the TM_{101}, which is the one commonly used for the design of spherical cavity filters [8]. In this paper, however, the spherical TE_{101} mode is instead used. In Fig. 2, the field distribution of both the fundamental mode TM_{101} and the higher order mode TE_{101} is shown. As can be seen, the electric field of the mode TE_{101} is concentrated around the center of the cavity forming a circular pattern. The concentration of the field reduces the currents on the cavity wall, thus resulting in a very high Q-factor. For example, for a cavity made of aluminum, the resulting Q-factor is about 23000 at 10 GHz, whereas the Q-factor of the fundamental mode resonating at the same frequency in an aluminum spherical cavity is 13800. For obtaining the same resonant frequency for the TM_{101} and the TE_{101}, the radius of the TE_{101} cavity is 1.61 times that of the TM_{101} cavity. The increasing of the radius also brings the advantage of improving the manufacturing tolerances. This is particularly useful when filters at high frequencies are considered, especially considering that at high frequencies, dimensions are not a problem. Furthermore, this feature is very interesting for very narrow-band filters where very high Q-factors are needed.

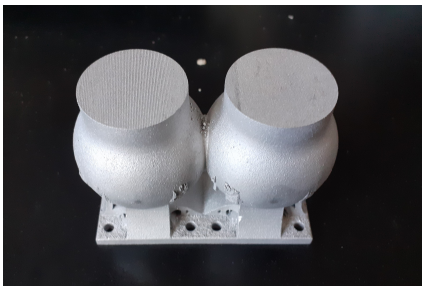

(a)

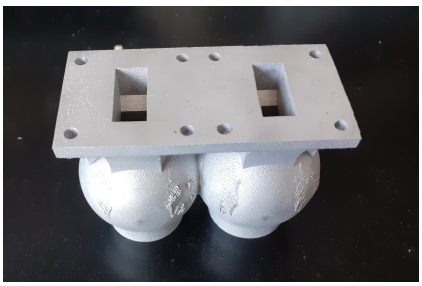

(b)

Fig. 3. Photos of a manufactured filter. (a) bottom view, (b) top view.

The resonance frequency of the spherical mode TE_{101} can be analytically evaluated by using the following equation:

$$f_r = \frac{u_{np}}{2\pi a\sqrt{\epsilon\mu}}, \tag{1}$$

where u_{np} are the roots of the Bessel functions. For example, for a radius of 21.1 mm, we obtain a resonance frequency of 10.167 GHz (where u_{np} is 4.493). This result has been verified by using the commercial software ANSYS HFSS, obtaining a resonant frequency of 10.162 GHz with a Q-factor of 23000 (using aluminum based on an ideal electrical conductivity of 33 MS/m).

III. 2-Pole Filter Design

A 3-D view of a two-pole filter is shown in Fig. 1. It consists of two resonators interconnected through an aperture. The second aperture of each cavity is rotated 90° with respect to the first along the E-plane. The initial radius of the cavity can be obtained by using eq. (1). A first draft design has been obtained from the synthesized filter, and then optimized to obtain the desired response. Once the geometry has been defined, a co-engineering approach has been exploited in order to make the geometry compatible with the AM process [10]. In particular, the cavity profile, as well as the coupling iris have been slightly modified in order to allow a vertical positioning of the filter, thus improving the manufacturing tolerances.

IV. Manufacturing and Measurements

Two prototypes have been manufactured in AlSi10Mg alloy by SLM process. The external supports have been applied only for the WR90 flanges. In Fig. 3, photos of manufactured prototypes are shown. A post processing process based on stress relieving and shot-peening has been carried out.

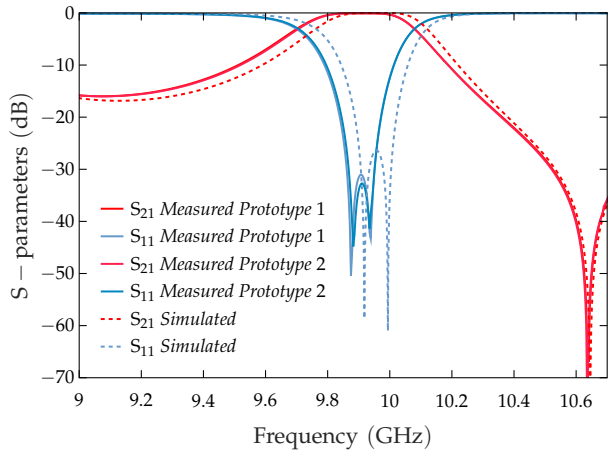

Fig. 4. Comparison between measured (continuous curve) and simulated (dashed curves) frequency response of the realized filters. Two prototypes in AlSi10Mg have been manufactured in SLM.

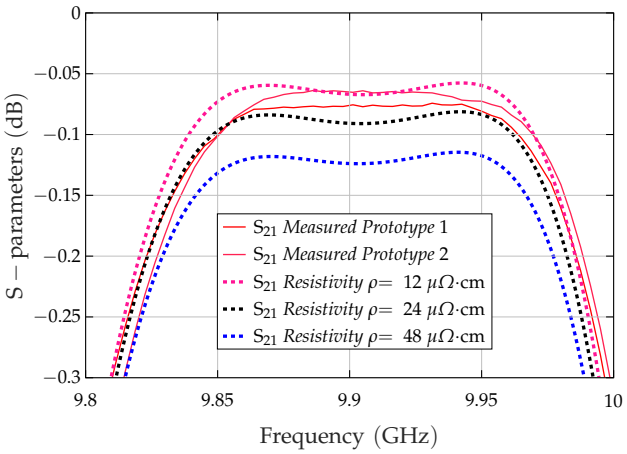

Fig. 5. Comparison between measured (continuous curves) and simulated (dashed curves) transmission coefficient in the passband. The measurements refer to two prototypes; the simulations have been carried out by considering different values of metal resistivity ρ.

Fig. 4 shows a comparison between the measured and simulated reflection and transmission coefficients of the filter. From the curves, it can be noticed a frequency shift of 45 MHz and a good repeatability of the manufacturing process. In order to derive the effective resistivity of the two prototypes, that takes into account the roughness of the alloy conductivity, a parametric analysis has been carried out by considering different values of ρ: 12 $\mu\Omega$·cm, 24 $\mu\Omega$·cm and 48 $\mu\Omega$·cm. For an easier comparison, the frequency shift of 45 MHz has been applied on the simulated curves. Fig. 5 reports a zoom of the transmission coefficient in the passband [9.8,10] GHz, proving that an equivalent resistivity between 12 and 24 $\mu\Omega$·cm is obtained. These values are in accordance with [10], [11], where for different devices, a value of around 16 $\mu\Omega$·cm was obtained. The measured insertion loss at midband is 0.07 dB, and 0.1 dB at cut edges of the filter, corresponding to a Q-factor of about 4500 for both prototypes. The return loss is higher than 30 dB, and no tuning elements have been employed.

V. Conclusions

TE_{101} spherical mode filters have been presented. The proposed filters have the advantage of high Q-factors. Two filter prototypes were manufactured by SLM 3-D printing process. Each filter was manufactured in a single piece, without the need of post assembling work. The measured narrow-band responses of the two prototypes show a high Q-factor with almost identical responses over the frequency band, thus demonstrating the repeatability of the process. No tuning screws have been used.

Acknowledgment

This work was supported by funds from the European Union's Horizon 2020 research and innovation programme under the Marie Skłodowska-Curie grant agreement No 811232.

References

[1] R. V. Snyder, G. Macchiarella, S. Bastioli, and C. Tomassoni, "Emerging trends in techniques and technology as applied to filter design," *IEEE Journal of Microwaves*, vol. 1, no. 1, pp. 317–344, 2021.

[2] S. Bastioli, C. Tomassoni, and R. Sorrentino, "A new class of waveguide dual-mode filters using TM and nonresonating modes," *IEEE Transactions on Microwave Theory and Techniques*, vol. 58, no. 12, pp. 3909–3917, 2010.

[3] C. Tomassoni, S. Bastioli, and R. Sorrentino, "Generalized TM dual-mode cavity filters," *IEEE Transactions on Microwave Theory and Techniques*, vol. 59, no. 12, pp. 3338–3346, 2011.

[4] V. Nocella, L. Pelliccia, C. Tomassoni, and R. Sorrentino, "Miniaturized dual-band waveguide filter using TM dielectric-loaded dual-mode cavities," *IEEE Microwave and Wireless Components Letters*, vol. 26, no. 5, pp. 310–312, 2016.

[5] C. Tomassoni, O. A. Peverini, G. Venanzoni, G. Addamo, F. Paonessa, and G. Virone, "3D printing of microwave and millimeter-wave filters: Additive manufacturing technologies applied in the development of high-performance filters with novel topologies," *IEEE Microwave Magazine*, vol. 21, no. 6, pp. 24–45, 2020.

[6] G. Venanzoni, M. Dionigi, C. Tomassoni, and R. Sorrentino, "3-D-printed quasi-elliptical evanescent mode filter using mixed electromagnetic coupling," *IEEE Microwave and Wireless Components Letters*, vol. 28, no. 6, pp. 497–499, 2018.

[7] E. López-Oliver and C. Tomassoni, "3-D-printed dual-mode filter using an ellipsoidal cavity with asymmetric responses," *IEEE Microwave and Wireless Components Letters*, pp. 1–1, 2021.

[8] C. Guo, X. Shang, M. J. Lancaster, and J. Xu, "A 3-D printed lightweight X-band waveguide filter based on spherical resonators," *IEEE Microwave and Wireless Components Letters*, vol. 25, no. 7, pp. 442–444, 2015.

[9] F. Zhang, C. Guo, Y. Zhang, Y. Gao, B. Liu, M. Shu, Y. Wang, Y. Dong, M. J. Lancaster, and J. Xu, "A 3-D printed bandpass filter using TM-mode slotted spherical resonators with enhanced spurious suppression," *IEEE Access*, vol. 8, pp. 213 215–213 223, 2020.

[10] O. A. Peverini, M. Lumia, F. Calignano, G. Addamo, M. Lorusso, E. P. Ambrosio, D. Manfredi, and G. Virone, "Selective laser melting manufacturing of microwave waveguide devices," *Proceedings of the IEEE*, vol. 105, no. 4, pp. 620–631, 2017.

[11] G. Addamo, O. A. Peverini, D. Manfredi, F. Calignano, F. Paonessa, G. Virone, R. Tascone, and G. Dassano, "Additive manufacturing of Ka-band dual-polarization waveguide components," *IEEE Transactions on Microwave Theory and Techniques*, vol. 66, no. 8, pp. 3589–3596, 2018.